www.czasopisma.pan.pl PAN www.journals.pan.pl

ARCHIVES of FOUNDRY ENGINEERING

ISSN (2299-2944)
Volume 18
Issue 1/2018

162 – 166

30/1

DOI: 10.24425/118831

Published quarterly as the organ of the Foundry Commission of the Polish Academy of Sciences

Copper in Ausferritic Compacted Graphite Iron

G. Gumienny *, B. Kacprzyk
Department of Materials Engineering and Production Systems, Lodz University of Technology,
Stefanowskiego 1/15 Street, 90-924 Łódź, Poland
*Corresponding author: Email address: grzegorz.gumienny@p.lodz.pl

Received 12.07.2017; accepted in revised form 04.10.2017

Abstract

This paper shows how it is possible to obtain an ausferrite in compacted graphite iron (CGI) without heat treatment of castings. Vermicular graphite in cast iron was obtained using Inmold technology. Molybdenum was used as alloying additive at a concentration from 1.6 to 1.7% and copper at a concentration from 1 to 3%. It was shown that ausferrite could be obtained in CGI through the addition of molybdenum and copper in castings with a wall thickness of 3, 6, 12 and 24 mm. Thereby the expensive heat treatment of castings was eliminated. The investigation focuses on the influence of copper on the crystallization temperature of the graphite eutectic mixture in cast iron with the compacted graphite. It has been shown that copper increases the eutectic crystallization temperature in CGI. It presents how this element influences ausferrite microhardness as well as the hardness of the tested iron alloy. It has been shown that above-mentioned properties increases with increasing the copper concentration.

Keywords: Theory of crystallization, Compacted graphite iron, Ausferrite, DTA method

1. Introduction

Among the modern varieties of cast iron, cast iron with compacted graphite occupies a special place of growing interest. This is due to its advantages in combining the benefits of gray and ductile cast iron. The most important are the vibration damping abilities as well as the high resistance to dynamic temperature changes. The shape of compacted graphite is covered by PN-EN ISO 945-1: 2008 and it is shown in Figure 1.

In accordance with PN-EN 16079: 2012 compacted graphite iron (CGI) shall contain 80% minimum type III graphite.

The rest of separations may be characterized by the type IV, V and VI in accordance with PN-EN ISO 945-1:2008.

.

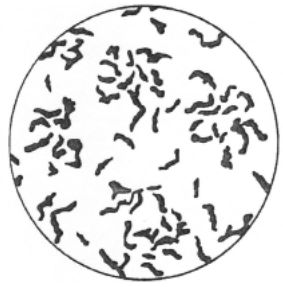

Fig. 1. The shape of graphite in cast iron - type III (according to PN-EN ISO 945-1:2008)

The standard specifies five grades CGI with a tensile strength of 300 to 500 MPa at an elongation from 2.0 to 0.5%, respectively (Table 1)

The grades of CGI are presented in Table 1.

Table 1.
The grades of CGI according to PN-EN 16079:2012

Symbol	Mechanical properties			
	R_m, MPa min.	$R_{p0,2}$, MPa min.	A, % min.	HBW
EN-GJV-300	300	210	2.0	140 to 210
EN-GJV-350	350	245	1.5	160 to 220
EN-GJV-400	400	280	1.0	180 to 240
EN-GJV-450	450	315	1.0	200 to 250
EN-GJV-500	500	350	0.5	220 to 260

The cast iron matrix changes from the predominantly ferritic (EN-GJV-300) to the pearlitic (EN-GJV-500).

The change of the matrix microstructure can be caused by modification of the chemical composition. Data concerning the influence of alloying additives on the CGI matrix can be found in papers [1-4].

Worldwide literature includes data concerning the possibility to obtain an ausferrite in CGI. It is usually obtained by heat treatment of castings [5-10]. This cast iron is referred to as AVI (Austempered Vermicular Iron). However, there is no data concerning the possibility to obtain an ausferrite in CGI without heat treatment.

Accordingly, the aim of this study is to investigate the possibility to obtain ausferrite from CGI through modification of its chemical composition. For the tests castings with a 3, 6, 12, 24 mm wall thickness were used. The castings were cooled inside the mould.

2. Methodology

Metal was melted in an electric medium-frequency induction crucible furnace of 30 kg capacity. Compacted graphite was obtained using Inmold technology. Schematic layout of elements in the mould is presented in Figure 2.

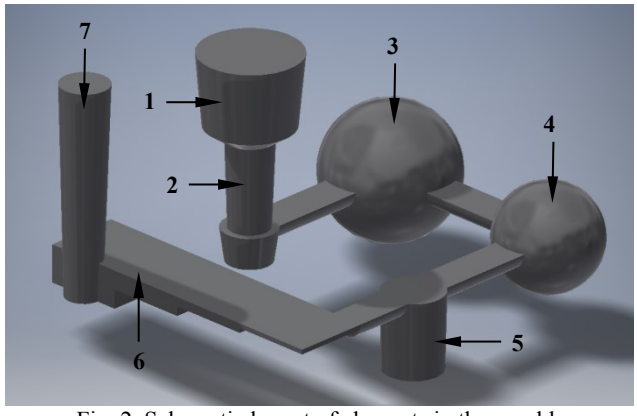

Fig. 2. Schematic layout of elements in the mould:
1 – pouring cup, 2 – downsprue, 3 – reaction chamber,
4 – mixing chamber, 5 – control chamber, 6 – stepped test casting,
7 – flow off

The pouring temperature was approx. 1480°C. The cast iron from the downsprue (2) flowed to the reaction chamber (3) where the master alloy was placed. Its chemical composition is shown in Table 2. The liquid alloy passed through the mixing chamber (4) and poured to the control chamber (5). In its thermal center, the PtRh10-Pt thermocouple (type S) was located to record the cooling as well as the crystallization process. Next the mould cavity (6) was filled with liquid iron and any excess escaped into the flow off (7). The tested casting was characterized by the wall thickness 3, 6, 12 and 24 mm.

Table 2.
The chemical composition of the master alloy

Chemical composition, wt%					
Si	Mg	Ca	La	Al	Fe
44÷48	5÷6	0.4÷0.6	0.25÷0.40	0.8÷1.2	rest

Magnesium and lanthanum were used as the nodulizers in the master alloy. There are calcium and aluminum as inoculants, while silicon is a graphite-forming element.

The chemical composition of CGI tested is presented in Table 3.

Table 3.
The chemical composition of CGI tested

No.	Chemical composition, wt%				
	C	Si	Mn	Mo	Cu
1.	3.57	2.60	0.03	1.71	1.01
2.	3.44	2.68	0.04	1.70	1.49
3.	3.54	2.64	0.04	1.67	1.96
4.	3.38	2.56	0.04	1.68	2.40
5.	3.82	2.40	0.03	1.60	2.90

Technically pure molybdenum and copper were used as alloying additives. Molybdenum at a concentration from about 1.6 to 1.7% significantly increased the austenite stability in the pearlitic area. It enabled the ausferrite to be obtained during continuous cooling. Cast iron hardenability was controlled by copper concentration in the range of 1-3%. In CGI with Mo and without copper, besides the ausferrite, ferrite and perlite also appeared. The concentration of magnesium in the cast iron ranged from 0.017 to 0.021%. The change in Mg concentration was dictated by the negative effect of copper on the graphite shape. Specimens for metallographic studies were cut from the central part of the stepped casting. After grinding and polishing they were etched with a 4% HNO_3 solution in C_2H_5OH. The Nikon Eclipse MA200 optical microscope and magnification ×500 were used to the metallographic examinations.

Microhardness was measured on the specimens with a wall thickness of 12 mm using the HV-1000B microhardness tester under a load of 0.9807 N according to PN EN ISO 6507-1.

The hardness of the cast iron was examined on specimens cut-off from the casting with wall thickness of 24 mm using the HPO-2400 hardness tester under a test load of 1840 N, a ball of diameter 2.5 mm and the dwell time 15 s.

3. Results

Figure 3 shows the DTA curves of ausferritic CGI containing approximately 1.7% Mo and 1% Cu.

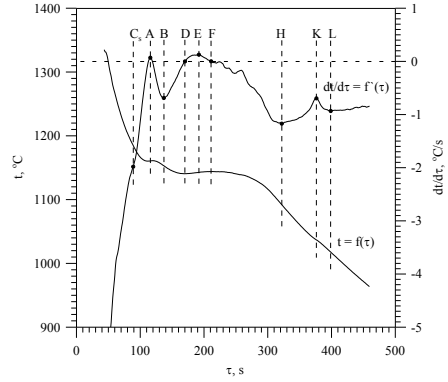

Fig. 3. The representative DTA curves of CGI containing approximately 1.7% Mo and 1% Cu

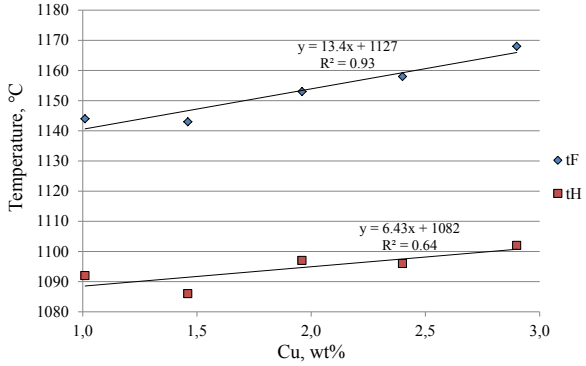

Fig. 4. The temperature of the eutectic transformation vs Cu concentration in ausferritic CGI

There are three thermal effects described by characteristic points on the DTA curves. C_sAB thermal effect comes from the transformation of a liquid into the primary austenite. The transformation of the liquid into the eutectic mixture of vermicular graphite and austenite causes DEFH thermal effect. Due to the positive segregation of Mo the liquid is strongly enriched in this element at the end of its crystallization, therefore its crystallization follows according to the metastable system. Therefore, the last thermal effect (HKL) comes from the crystallization of the ledeburitic carbides. Crystallization of the cast iron finishes at 1018°C (point L). The change in Cu concentration in ausferritic CGI did not cause the form of the DTA curves. On the other hand, it has changed the temperature of the phase transformations. In Table 4 the temperature of the phase transformations in ausferritic CGI is presented.

Table 4.
The temperature of the phase transformations in ausferritic CGI

Cu,	t, °C								
wt%	tC_s	tA	tB	tD	tE	tF	tH	tK	tL
1.01	1185	1161	1153	1141	1143	1144	1092	1037	1018
1.49	1219	1197	1175	1137	1139	1143	1086	1034	1008
1.96	1195	1168	1160	1150	1151	1153	1097	1042	1019
2.40	1198	1169	1160	1145	1147	1158	1096	1043	1017
2.90	1205	1171	1168	1165	1167	1168	1102	1044	1025

From the data presented in Tab. 4 results that the copper in the tested cast iron increases the maximum temperature of the eutectic transformation (point F, Fig. 3) and the temperature of the crystallization finish of the graphite eutectic (point H, Fig. 3). There was no significant effect of this element on the crystallization temperature of the carbide eutectic (point L, Fig. 3). The influence of copper on the eutectic transformation temperature is presented graphically in Figure 4.

Fig. 4 shows that copper increases the maximum eutectic transformation temperature (tF) by about 13°C per 1% Cu and the crystallization temperature of the graphite eutectic (tH) by about 6°C per 1% Cu.

Figure 5 (a, b) shows the microstructure of the ausferritic CGI containing about 1.7% Mo and 1% Cu in castings with a wall thickness of 3 mm (a) and 24 mm (b).

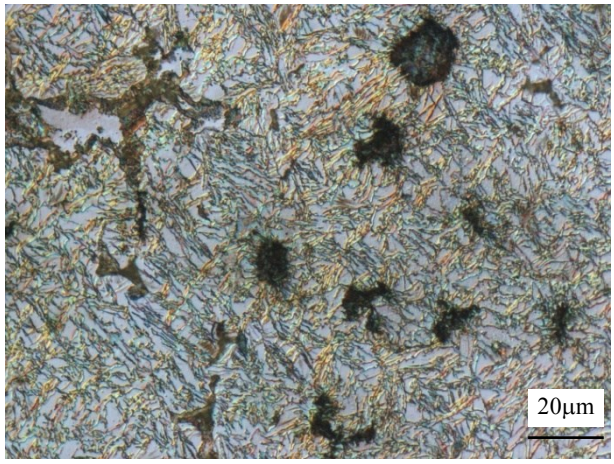

a) microstructure: compacted graphite, ausferrite, carbides, pearlite

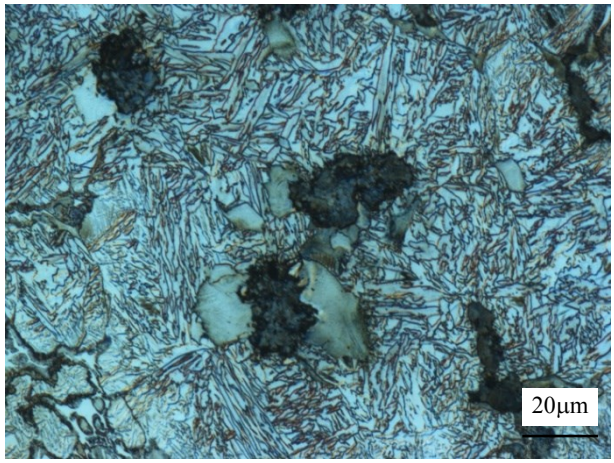

b) microstructure: compacted graphite, ausferrite, ferrite, carbides, pearlite

Fig. 5 (a, b). The microstructure of compacted graphite iron containing approximately 1.7% Mo and 1% Cu in: a) 3 mm; b) 24 mm castings wall thickness

From the results shown in Fig. 5, the microstructure from a 3 mm wall thick cast consists of vermicular graphite, ausferrite, as well as small-scale carbides on the grain boundaries. Most likely,

they are molybdenum-containing carbides. There is a small amount of perlite near to carbides. The increase in wall thickness up to 24 mm resulted in the appearance of ferrite at the graphite as a result of the lower cooling rate.

Figure 6 (a, b) shows the microstructure of the ausferritic CGI containing about 1.7% Mo and 1.5% Cu. This is from castings with a wall thickness of 3 mm (a) and 24 mm (b).

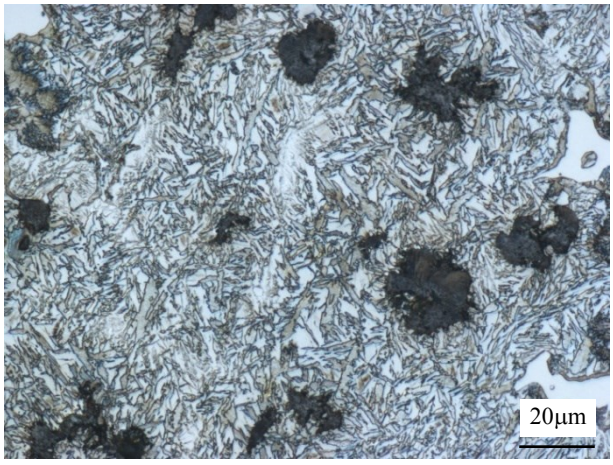

a) microstructure: compacted graphite, ausferrite, carbides, pearlite

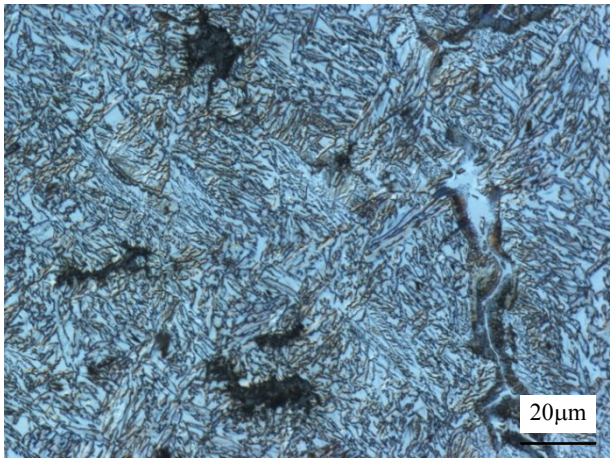

b) microstructure: compacted graphite, ausferrite, carbides, pearlite

Fig. 6 (a, b). The microstructure of compacted graphite iron containing approximately 1.7% Mo and 1.5% Cu in: a) 3 mm; b) 24 mm castings wall thickness

The increase in Cu concentration up to 1.5% resulted in the lack of ferrite on the grain boundaries. There was no change in the morphology of the bainitic ferrite plates. There was also no significant change in the surface area of carbides.

The increase in Cu concentration up to about 2% did not significantly affect the microstructure of the cast iron matrix. The surface area of the carbides was only slightly reduced. A further increase in copper concentration up to about 2.4-2.9% resulted in the appearance of plates characteristic for the lower ausferrite.

The microstructure of CGI containing about 1.7% Mo and 2.9% Cu in castings with a wall thickness of 3 mm and 24 mm is shown in Figure 7 (a, b).

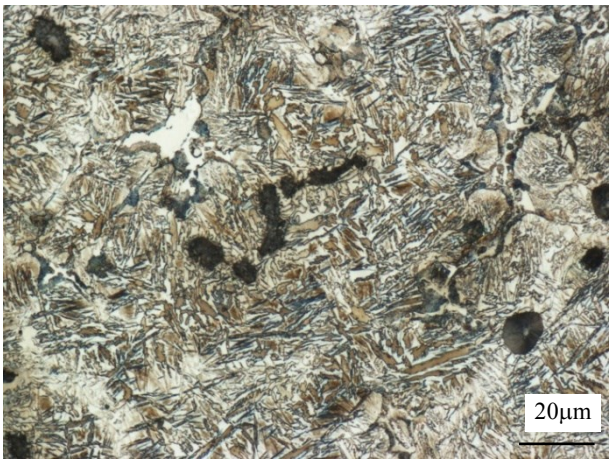

a) microstructure: compacted graphite, ausferrite, carbides, pearlite

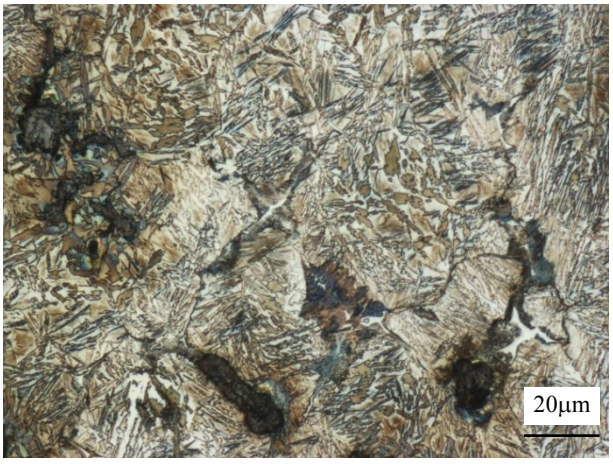

b) microstructure: compacted graphite, ausferrite, carbides, pearlite

Fig. 7 (a, b). The microstructure of compacted graphite iron containing approximately 1.7% Mo and 3% Cu in: a) 3 mm; b) 24 mm castings wall thickness

From the data presented in Figure 7b, the increase in Cu concentration to 3% resulted in an almost total disappearance of carbides when using 24 mm thick walled castings.

The effect of copper on the ausferrite microhardness in CGI is shown in Figure 8.

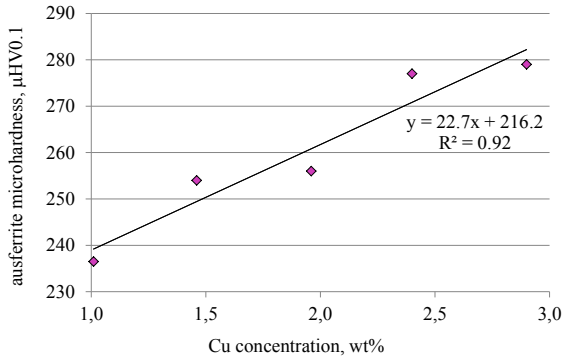

Fig. 8. Ausferrite microhardness vs Cu concentration in CGI

Fig. 8 shows that copper increases the hardness of ausferrite in cast iron with vermicular graphite by about 23 µHV per 1% of concentration. This is probably due to the increase in hardenability of the cast iron, and therefore the amount of lower ausferrite.

The hardness of ausferritic CGI vs. copper concentration is presented in Figure 9.

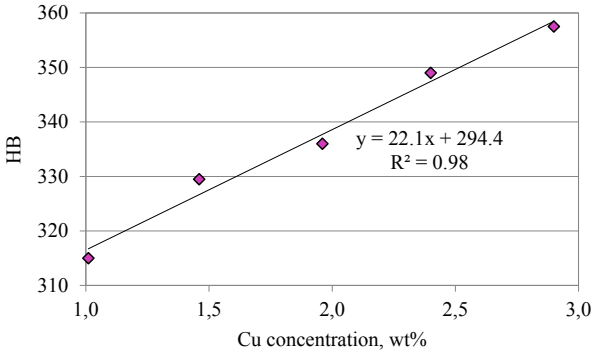

Fig. 9. CGI hardness vs Cu concentration

From Figure 9 it appears that the increase in copper concentration results in an increase in the CGI hardness by about 22 HB per 1% concentration. At the initial stage (from 1 to 1.5% Cu) it is caused by both the ferrite disappearance and an increase in the ausferrite microhardness. When the copper concentration is higher, the reason is only the second of the above-mentioned factors.

4. Conclusions

The results of the research predestine to the following conclusions:

- it is possible to obtain an ausferrite in CGI castings with a wall thickness of 3, 6, 12 and 24 mm without heat treatment. This is through the addition of Mo and Cu at concentrations from approximately 1.6 to 1.7% and from 1.5 to 3% respectively,
- copper in ausferritic CGI increases the maximum eutectic transformation temperature by about 13°C per 1% Cu and the crystallization finish temperature of the graphite eutectic mixture by approx. 6°C per 1%,
- copper increases the ausferrite microhardness by about 23 µHV per 1% of concentration,
- Cu increases the hardness of ausferritic CGI by about 22 HB per 1% of concentration.

References

[1] Guzik, E. & Kleingartner, T. (2009). A study on the structure and mechanical properties of vermicular cast iron with pearlitic-ferritic matrix. *Archives of Foundry Engineering*. 9(3), 55-60.

[2] Popov, P.I. & Sizov, I.G. (2006). Effect of Alloying Elements on the Structure and Properties of Iron with Vermicular Graphite. *Metal Science and Heat Treatment*. 48(5-6), 272-275.

[3] Zhou, G. & Liu, W. (2008). Production technique of vermicular graphite iron cylinder head of vehicle diesel engine. *China Foundry. Special Review*. 5(3), 153-161.

[4] Choong-Hwan, L. & Byeong-Choon, G. (2011). Development of compacted vermicular graphite cast iron for railway brake discs. *Metals and Materials International.* 17(2), 199-205. DOI: 10.1007/s12540-011-0403-x.

[5] Soiński, M.S. & Jakubus, A. (2014). Initial Assessment of Abrasive Wear Resistance of Austempered Cast Iron with Vermicular Graphite. *Archives of Metallurgy and Materials*. 59(3), 1073-1076.

[6] Andrsova, Z. & Volesky, L. (2012). The Potential of Isothermally Hardened Iron with Vermicular Graphite. COMAT 2012. 21.-22. 11. 2012. Plzeň, Czech Republic, EU. Retrieved May, 25. 2015 from http://www.comat.cz/files/-proceedings/11/reports/1060.pdf.

[7] Pytel, A. & Gazda, A. (2014). Evaluation of Selected Properties in Austempered Vermicular Cast Iron (AVCI). *Transactions of Foundry Research Institute*. LIV(4), 23-31. DOI: 10.7356/iod.2014.18.

[8] García-Hinojosa, J.A., Amaro A.M., Márquez, V.J. & Ramírez-Argaez, M.A. (2007). Manufacturing of Carbide Austempered Vermicular Iron. METAL 2007. 22. – 24. 5. 2007 Hradec nad Moravicí. Retrieved April, 10. 2017 from http://konference.tanger.cz/data/metal2007/sbornik/Lists/Papers/120.pdf.

[9] Mierzwa, P. & Soiński, M.S. (2010). The effect of thermal treatment on the mechanical properties of vermicular cast iron. *Archives of Foundry Engineering*. 10(1), 99-102.

[10] Ramadan, M., Nofal, A.A., Elmahalawi, I. & Abdel-Karim, R. (2006). Comparison of austempering transformation in spheroidal graphite and compacted graphite cast irons. *International Journal of Cast Metals Research*. 19(3), 151-155.